Carbohydrate Polymers 254 (2021) 117434

Contents lists available at ScienceDirect

Carbohydrate Polymers

journal homepage: www.elsevier.com/locate/carbpol

In vitro biological response of human osteoblasts in 3D chitosan sponges with controlled degree of deacetylation and molecular weight

Mousumi Sukul [a,*], Priyanka Sahariah [b], Hélène L. Lauzon [c], João Borges [d], Már Másson [b], João F. Mano [d], Håvard J. Haugen [a], Janne E. Reseland [a]

[a] Department of Biomaterials, Institute of Clinical Dentistry, University of Oslo, 0317 Oslo, Norway
[b] Faculty of Pharmaceutical Sciences, School of Health Sciences, University of Iceland, Hofsvallagata 53, IS-107 Reykjavík, Iceland
[c] Primex ehf, Óskarsgata 7, 580-Siglufjordur, Iceland
[d] Department of Chemistry, CICECO – Aveiro Institute of Materials, University of Aveiro, Campus Universitário de Santiago, 3810-193 Aveiro, Portugal

ARTICLE INFO

Keywords:
Chitosan
Degree of deacetylation
Molecular weight
Osteoblasts

ABSTRACT

We have studied the effect of chitosan sponges, produced from chitosan batches with distinct degree of deacetylation (DDA) and molecular weight (*Mw*), on the adhesion, growth and differentiation of primary human osteoblasts with an aim to offer a suitable tool for guided bone regeneration. All the chitosan sponges revealed similar microstructure, irrespective of the DDA (58, 73, 82, 88, and 91 %) and *Mw* (749, 547, 263, 215, and 170 kDa, respectively). Cell spreading was higher on sponges having a higher DDA. Higher DDA induced a more pronounced increase in alkaline phosphatase activity, osteopontin (OPN), vascular endothelial growth factor-A (VEGF), interleukin-6 (IL-6), and reduction in monocyte chemoattractant protein-1 (MCP-1), sclerostin (SOST) and dickkopf related protein-1 as compared to lower DDA. Lower DDA induced the increased secretion of osteoprotegerin and SOST as compared to higher DDA. The combination of higher DDA and *Mw* induced an increased secretion of VEGF and IL-6, however reduced the secretion of OPN as compared to chitosan with similar DDA but with lower *Mw*. In summary, the variations in cellular responses to the different chitosan sponges indicate a potential for individual tailoring of desired responses in guided bone regeneration.

1. Introduction

Three-dimensional (3D) porous structures serve to provide a suitable environment to promote cell ingrowth, incorporation of cells and secreted growth factors to the surrounding tissue for guided bone regeneration (Eiselt et al., 2000; Hollister, 2005; Liu Tsang & Bhatia, 2004). A highly porous scaffold with interconnected pores is beneficial for the exchange of nutrients and oxygen essential for cell survival (Loh & Choong, 2013). In addition, the mechanical properties of the developed scaffolds constitute an important feature to maintain their structural integrity (Zhao et al., 2018). Techniques, such as, freeze-drying, sponge replication, 3D printing, have been adopted to develop 3D scaffolds of various materials, such as polymers, ceramics, and composites, with the desirable properties (Kumar et al., 2020; Liu et al., 2020; Wang et al., 2020).

Chitosan is the second most naturally abundant polysaccharide, which is obtained from the crustaceans exoskeleton (crab/shrimp), fungi cell walls, and cuticles of insects after the deacetylation of chitin (Austin et al., 1981; Cho, No, & Meyers, 1998). Chitosan is documented to entail biocompatibility, biodegradability and antimicrobial properties (Alves & Mano, 2008; Chandy & Sharma, 1990; Croisier & Jérôme, 2013; Di Martino, Sittinger, & Risbud, 2005; Khor & Lim, 2003). It has structural similarity to the extracellular matrix glycosaminoglycans and provides a supportive matrix for cell ingrowth and proliferation in porous, particle or membranous forms (Custódio et al., 2015; Francis Suh & Matthew, 2000; Garcia Cruz et al., 2010). Chitosan forms gels in the presence of physical or chemical crosslinkers (Berger et al., 2004; Monteiro & Airoldi, 1999; Muzzarelli, 2009), which makes it an attractive injectable hydrogel for tissue engineering applications (Chenite et al., 2000; Costa & Mano, 2015; Hoemann et al., 2005). Due to the polycationic linear structure of chitosan at pH below pKa (~6.2–6.5) (Cheung et al., 2015), it binds negatively charged counterparts, including proteins on its surface. Protein adsorption and subsequent cell adhesion on biomaterial surface is the essential prerequisite for biomaterial induced tissue healing (Zaharoff et al., 2007). In addition, drug delivery applications with bioactive molecules, like TGF-β1

* Corresponding author.
E-mail address: mousumi.sukul@odont.uio.no (M. Sukul).

https://doi.org/10.1016/j.carbpol.2020.117434
Received 20 May 2020; Received in revised form 3 October 2020; Accepted 19 November 2020
Available online 22 November 2020

and BMP-2/TGF-β2, incorporated in chitosan have been tested (Han et al., 2014, 2017; Li et al., 2014; Rezaii, Oryan, & Javeri, 2019).

Chitosan has been reported as an antimicrobial agent against a wide range of microorganisms, as cationic chitosan molecules bind with anionic microbial phospholipid cell membranes. This interaction alters the membrane permeability resulting in osmotic imbalance, suppressed biosynthesis and eventually the death of the organism (Rabea et al., 2003). In biological systems, chitosan is mainly degraded by enzymatic digestion. Lysozymes primarily cause the degradation of chitosan through the hydrolysis of glucosamine-glucosamine and N-acetyl-glucosamine linkages (Kean & Thanou, 2010). Degraded chitosan oligomers triggers humoral response by activating macrophages to produce interferon, TNF and interleukin-l (Muzzarelli, 1993).

Chitosan exhibits distinct structural features while varying the degree of deacetylation (DDA), molecular weight (M_W), degree of crystallinity, and distribution of acetyl groups (Li et al., 1992). The process of deacetylation leads to the removal of acetyl groups on chitin side chains, revealing the amino groups via alkaline treatment. The DDA of chitosan typically varies from 50 % to 95 % but a DDA higher than 95 % can be obtained through further deacetylation steps. The DDA may influence the physiochemical characteristics, such as, crystallinity, surface roughness, hydrophobicity, degradation, and material strength of chitosan structures (Foster et al., 2015). The effect of chitosan with different percentage of DDA on cellular response of different cell lineage has been assessed. Chatelet et al. observed that the keratinocyte adhesion and proliferation increased while increasing the DDA of chitosan films. Fibroblasts adhered twice as much as keratinocytes on these film but did not proliferate. The authors claimed that extremely high adhesion on this material inhibited the cell growth (Chatelet, Damour, & Domard, 2001). Moreover, Wenling et al. reported that the chitosan films with higher DDA provided better substrata for Schwann cell spreading and proliferation, and a DDA higher than 90 % is considered promising for peripheral nerve regeneration (Wenling et al., 2005). Leider et al. found that higher DDA chitosan membranes facilitated the attachment and proliferation of MC3T3-E1 cells without inducing spontaneous osteogenic differentiation (Lieder et al., 2012). The molecular weight (M_W) is another important factor that determines the properties and functions of chitosan. It was reported that an increase in M_W resulted in an increased tensile strength of chitosan membranes (Rong Huei & Hwa, 1996) but decreased biodegradation of the biopolymer (Zhang & Neau, 2001). Hamilton et al. cultured normal human osteoblasts (NHOst) on different chitosan films with DDA ranging from 76 to 96% and viscosity-average *Mw* ranging from 2400 to 8200 kDa. They did not identify any relationship between DDA and *Mw* on cell growth and proliferation (Hamilton et al., 2007). Hsu et al. reported that immortalized rat chondrocytes had an higher cell adhesion and proliferation on chitosan films with higher DDA and lower average M_W (Hsu et al., 2004). However, to date, most of the studies investigating the influence of DDA and M_W were done in 2D, which do not resemble the 3D microenvironment of native extracellular matrix.

Herein, we investigated the effects of both the DDA and M_W of 3D chitosan sponges on the growth and differentiation of primary human osteoblasts. Porous sponges were created by freeze-drying and the cell behavior was studied using non-osteogenic media, to evaluate the osteoinductive properties. To the best of our knowledge, this is the first in-detail report on the secretion of different bone markers and cytokines from human osteoblasts in response to the 3D sponges, which offers a promising route for guided bone regeneration.

2. Materials and methods

2.1. Chitosan powders

The characterization of the various batches of chitosan powders (ChitoClear®) obtained from Primex ehf (Siglufjordur, Iceland) are presented in Table 1. Chitosan powders were sterilized by autoclaving at 121 °C for 20 min (Bhattacharya et al., 2012). Measurements of DDA, *Mw* and dispersity were determined using autoclaved chitosan samples.

Table 1
Properties of different chitosan batches (autoclaved).

Sample name	DDA (%)	M_w (kDa)	Viscosity* (cP)	Dispersity	Endotoxin content* (EU/g)
CS58	58	749	824	1.92	<0.500
CS73	73	547	795	1.47	6.194
CS82	82	263	122	2.55	<0.500
CS88	88	215	749	3.12	8.075
CS91	91	170	14	4.25	<0.500

CS = chitosan, DDA = degree of deacetylation, M_w= weight average molecular weight, kDa = kilodalton, cP = centipoise.
* measured in non-autoclaved chitosan samples.

DDA of various chitosan batches were calculated from DA values obtained using ^{1}H-NMR spectroscopy. Aliquots of 10 mg chitosan powder was stirred in 0.5 % deuterium chloride solution (DCl) in deuterium oxide (D_2O) for 18 h at room temperature until fully dissolved. The degree of acetylation (DA) in % was then calculated from the integrals of the ^{1}H-NMR spectrum using the following equation:

$$DA = \left[\frac{\int (CH3C = O)}{\int (H2 - H6)}\right]\left[\frac{6}{3}\right] *100$$

Average of DA values from two measurements were taken as the final value. DDA was obtained by calculating % DDA = (1-DA)*100.

Weight average molecular weight (M_W) and dispersity ($Đ_M$ = Mw/Mn, where Mw is the weight average molecular weight and Mn is the number average molecular weight) were determined using gel permeation chromatography (GPC). GPC measurements were done using the Polymer Standards Service (PSS GmbH, Mainz, Germany), Dionex Ultimate 3000 HPLC system (Thermo Scientific-Dionex Softron GmbH, Germering, Germany), Dionex Ultimate 3000 HPLC pump and Dionex Ultimate 3000 autosampler (Thermo Scientific-Dionex Softron GmbH), Shodex RI-101 refractive index detector (Shodex/Showa Denko Europe GmbH, Munich, Germany), PSS's ETA-2010 viscometer and MALLS detector (PPC SLD 7100). WINGPC Unity 7.4 software (PSS GmbH) was used for data collection and processing. A series of three columns [PSS Novema 10 μ guard (50 × 8 mm), PSS Novema 10 μ 30 Å (150 × 8 mm) and PSS Novema 10 μ 1000 Å (300 × 8 mm)] (PSS GmbH) were used in the HPLC system. ReadyCal-Kit Pullulan standards with M_p (180–708,000 Da) from PSS GmbH were used for calibration. The eluent used was 0.1 M NaCl/0.1 % TFA solution. Each sample was dissolved in the same eluent as mentioned above at a concentration of 1 mg/mL at 25 °C using a flow rate of 1 mL/min. They were filtered prior to analysis using a syringe filter containing PTFE membrane with pore size 0.45 μm and 25 mm in diameter (Phenomenex, Torrance, CA, USA). The dn/dc was set to to 0.150 (Tiraferri et al., 2014). Each sample had an injection volume of 100 μL and a retention time of 30 min. All the measurements were done in triplicates.

Apparent viscosity of non-autoclaved chitosan powders (ChitoClear, Primex, Iceland) was assessed using acid-soluble chitosan solutions (1% (w/w) in 1% (v/w) glacial acetic acid (Honeywell Fluka, Germany) and determined with a Brookfield viscometer, model DV-II + Pro (Brookfield Engineering Labs., Middleboro, MA, USA). Chitosan quantity was corrected on a dry matter basis. Measurements were made using an appropriate spindle and speed (30 rpm, otherwise 60 rpm) in the solution (600 g) at 25 ± 0.2 °C and reported in centipoise (cP).

Endotoxin content of non-autoclaved chitosan powders were measured at Charles River Laboratories (Ecully, France). A 5 mg/mL solution was prepared in extracting fluid (LAL reagent, water pre-heated at 37 °C +/−1 °C). The solution was incubated at room temperature for 1 h, then centrifuged at 5000 rpm for 1 min. The supernatant was tested undiluted. Test was performed using "Endotoxin Specific buffer" (BG120).

2.2. Production of Chitosan sponges

Chitosan (2%, w/v) was dissolved in 1% acetic acid (Sigma-Aldrich, St Louis, Missouri, USA), poured into small polyethylene molds, and crosslinked with genipin (0.02 %, w/v) (Sigma-Aldrich) overnight on a shaker at room temperature. Crosslinked chitosan gels were frozen at −80 °C for 8 h and lyophilized at −80 °C overnight to produce 3D sponges. The prepared sponges were 10 mm in diameter and 2 mm thick.

2.3. Characterization of the chitosan sponges

2.3.1. Scanning electron microscopy (SEM)

The morphology of the chitosan sponges was examined by scanning electron microscope (SEM TM3030, Hitachi High-Technologies Europe GmbH, Krefeld, Germany). Briefly, chitosan sponges were sputter coated with gold and mounted on aluminum stubs with double-sided carbon conductive adhesive tape for electrical contact purposes. All images were taken in backscattered electron mode at an accelerating voltage of 15 kV.

2.3.2. Nano-computed tomography (NanoCT)

The morphometry of the sponges was analyzed using Nano-computed tomography (NanoCT). For scanning, a multiscale x-ray NanoCT Skyscan 2211 (Bruker MicroCT, Kontich, Belgium) was used, with a nanofocus x-ray tube set to work at 32 kV/340 μA. For all the scans, the acquisition parameters were: exposure time of 1200 ms with an averaging frame of 2; full rotation of 360° with a rotation step of 0.31°, resulting in a scanning time of about 50 min per sample and a final pixel size of 600 nm. The images were reconstructed with NRecon v.1.7.4.6 software (Bruker MicroCT) and finally CTAn v. 1.18.4.0 software (Bruker MicroCT) was used for the 3D morphometric analysis of the sponges.

2.3.3. Mechanical test

The compressive strength of all sponge groups were measured by using a uniaxial mechanical testing machine (Zwick/Roell Z2.5; Zwick GmbH & Co. KG, Ulm, Germany). Cylindrical sponges with 10 mm in diameter and 8 mm in height were compressed up to 70 % of their initial length at the testing speed of 1 mm/min with a 1 kN load cell. The compressive strength was calculated using the software testXpert II (Zwick/Roell).

2.3.4. Swelling ratio

Sponges with known weight (Wo) were soaked in deionized water and incubated at room temperature. The sponges were taken out at specific intervals, wiped with a filter paper to remove the excess water, and the weights (Ws) recorded (Stie et al., 2020). The swelling ratio was calculated as (Ws − Wo)/Wo.

2.3.5. Degradation

In vitro degradation rate of the sponges was determined by measuring the weight loss over time in PBS (Sigma-Aldrich, Missouri, USA) solution with and without 10 mg/mL lysozyme (hen egg white, Sigma-Aldrich, Missouri, USA) for 21 days. In brief, the initial weight of the sponges was recorded (Wi). The sponges were then submerged in PBS with and without lysozyme; and incubated at 37 °C. After specific intervals, the sponges were taken out, washed with deionized water, and freeze-dried. The dry weight of each sponge was recorded (Wd). The PBS solutions with and without lysozyme were replaced with fresh solution every other day. Degradation rate was calculated as:

Degradation (in % of initial weight) = ((Wi - Wd)/ Wi) x 100

2.4. Experimental design

Chitosan sponges were sterilized in a 70 % (v/v) ethanol solution for 6 h followed by washing 4 times in PBS (5 min each cycle). Then, the sponges were kept submerged in medium for approximately 30 min before cell seeding.

Normal Human Osteoblast cells (NHOst; Lonza, Basel, Switzerland) cultured in osteoblast growth medium (Promocell, Heidelberg, Germany) were used in the *in vitro* studies. The sponges seeded with cells at a density of 3×10^4 cells/cm^2 were incubated in the culture medium in 48 well culture plates and the medium was harvested on days 1, 3, 7, 14 and 21. Cells cultured at the same density on cell culture plates without sponges were used as control, enabling monitoring of the osteoblasts in a well characterized 2D set up. Five parallels of each chitosan sponge groups were tested.

2.5. Cell attachment and distribution

The attachment and spreading of cells on the sponges were studied after staining according to Kim et al. (Kim et al. (2014). Briefly, on day 3, the cell culture medium was harvested, and the cells on the sponges were washed twice with PBS, fixed in 4% paraformaldehyde for 10 min and washed with PBS. The cells were then permeabilized with 0.25 % Triton-X for 10 min and washed with PBS. A blocking solution of 2.5 % BSA (in PBS) was added to prevent non-specific binding. Next, the cells were stained with Alexa Fluor (568) conjugated Phalloidin (Thermo Fischer Scientific, 1:400 working dilution in PBS). Nuclei were stained with DAPI (Thermo Fischer Scientific, 1:1000 working dilution in PBS). Stained cells were observed under a confocal fluorescent microscope (Leica TCS SP8, Leica Microsystems, Wetzlar, Germany).

2.6. Lactate dehydrogenase activity

Cytotoxic effects of the sponges were evaluated by the lactate dehydrogenase activity (LDH) in the cell culture medium using cytotoxicity detection kit (Roche Diagnostics, Indianapolis, IN, USA) according to producer's instructions. Cell culture medium was harvested after 1, 3, 7, 14 and 21 days of incubation. Duplicates of 50 μl of sample were added to 50 μl of mixture (catalyst and dye solution) and incubated in the dark for 30 min before measuring the absorbance in an absorbance microplate reader (ELx800, BioTek, Vermont, USA) at a wavelength of 490 nm.

2.7. Caspase-3 activity

Csapase-3 activity in the cell culture media of osteoblasts cultured on the sponges were measured using Caspase-3 (Human) ELISA Kit (Milpitas, California, USA. Cell culture medium was harvested after 1, and 3 days of incubation, and aliquots (100 μl) was analyzed according to the manufacturer's protocol. The absorbance was measured using a microplate reader (BioTek El x 800, BioTek Instruments Inc., Winooski, VT, USA) at 450 nm.

2.8. Alkaline phosphatase activity

Alkaline phosphatase (ALP) activity was quantified by measuring the hydrolysis of p-nitrophenyl phosphate (pNPP, Invitrogen, Carlsbad, California, USA) at 405 nm. Standard curve prepared by using calf intestinal alkaline phosphatase (CIAP, Promega, Madison, Wisconsin, USA) was used as a reference. Aliquots of 25 μL of samples together with 100 μL of pNPP were incubated for 30 min at room temperature according to procedure (Riksen et al. (2011). The reaction was stopped with the addition of 50 μL of 3 M NaOH and the absorbance was read in the absorbance microplate reader.

2.9. Quantification of released bone markers and cytokines

The effect of the various chitosan sponges on the secretion of bone markers and cytokines to the culture medium was measured using Milliplex Human Bone Panel kit (OPG, OPN, SOST, DKK-1; EMD Millipore Corporation, Billerica, Massachusetts, USA) and Human Cytokine Panel kit (MCP-1, IL-6, VEGF; EMD Millipore Corporation) after 3, 7, 14 and 21 days of culture. All analyses were performed according to manufacturer's protocols. Multi-analyte profiling of the protein levels in cell culture medium was performed on the Luminex 200 system using xMAP technology (Luminex, Austin, Texas, USA). Acquired fluorescence data were analyzed by the xPONENT 3.1 software (Luminex).

2.10. Statistical methods

Statistical analysis was performed using SigmaPlot 14.0 (Systat Software Inc., Chicago, IL, USA). Student *t*-test was used to evaluate the effect of different chitosan sponges compared to control and between each group at each time point. Normality and equal variance tests were performed prior to the testing using Shapiro-Wilk and Brown-Forsythe, respectively. The Mann-Whitney Rank Sum Test was used if the results were not normally distributed. The significance level was set to $p \leq 0.05$.

3. Results

3.1. Properties of chitosan powders

The properties and the endotoxin content of different chitosan powders are presented in Table 1. In the gel permeation chromatography (GPC) analyses, the dn/dc value was set to 0.150, as in the previous work by Tiraferri et al. (Tiraferri et al. (2014). Other groups have used values ranging from 0.142 to 0.163 (Christensen, Vold, & Vårum, 2008; Muzzarelli, Lough, & Emanuelli, 1987; Rinaudo, Milas, & Le Dung, 1993). Due to practical consideration an average value for dn/dc was used, but this value can vary with DDA which may explain the difference between the molecular weight determined by GPC and viscometry. 0.1 M NaCl + 0.1 % TFA eluent was used as a mobile phase as recommended by the manufacturer of the column. Other studies have recommended the use of sodium acetate/acetic acid as mobile phase (Christensen et al., 2008; Rinaudo et al., 1993; Terbojevich et al., 1991). We have tested this solvent system, but the outcome was not affected.

The DDA of chitosan powders ranged from 58 % to 91 % and the molecular weight was inversely related to DDA ranging from 749 kDa to170 kDa. Viscosity of the powders with similar DDA, such as, CS88 and CS91 were notably different. The endotoxin content was very low in 3 out of 5 powders, and was not related to variations in DDA or Mw.

3.2. Characterization of chitosan sponges

SEM micrographs revealed that all chitosan sponge groups were highly porous with interconnected pores (Fig.1). Altering the DDA did not induce significant changes in the surface morphology of the chitosan sponges.

Nano CT analysis of sponges reveals a variation in pore size for the different chitosans, however, this failed to be significantly different between the groups. The average pore size of the sponges was 53–88 μm with the porosity ranging from 90 to 94% (Table 2). The average lamella thickness was around 5 μm for all sponge groups. The compressive strength of the sponges was inversely related to DDA (Table 2).

Swelling behavior of the sponges is presented in Fig. 2A. Water uptake was measured for up to 12 h (720 min). All the sponges swelled rapidly within the initial 30 min, and maintained a steady increase until the end of the test. Swelling ratio was higher in the sponges with higher DDA than the sponges with lower DDA. Degradation behavior of the sponges is presented in Fig. 2B and C. The initial degradation rate in lysozyme solution was slow for all the sponge groups. However, on day 14, sponges with lower DDA showed a much faster degradation rate than that of the sponges with higher DDA. On day 21, the degradation rate of CS58 and CS71 sponges were significantly lower than CS88 and CS91 ($p < 0.05$) (Fig. 2B). The degradation rate was considerably slower for all the sponge groups in PBS (Fig. 2C).

3.3. Cell morphology and cytotoxicity

Under confocal microscope inspection, the stained cells were localized at different depths of the sponges indicating cell ingrowth and growth over the pores (Fig. 3a–e). Cells on the sponges with the lowest DDA showed spherical shaped morphology, mostly clustered into spheroid-like aggregates (Fig. 3a). Generally, cell spreading was higher with the increase of DDA. However, there was a considerable difference in the attachment and colonization behavior between the sponges with higher DDA (CS88 and CS91). Less cells were attached on the surface of

Table 2
Characterization of sponges made from different chitosan batches.

Sample name	Porosity (%)	Pore size (μm)	lamella thickness (μm)	Compressive strength (MPa)
CS58	94 ± 0.48	76 ± 27	5.0 ± 1.5	0.037 ± 0.005
CS73	94 ± 0.47	88 ± 37	5.6 ± 1.9	0.040 ± 0.005
CS82	93 ± 0.49	77 ± 30	5.2 ± 1.6	0.038 ± 0.003
CS88	93 ± 0.74	85 ± 34	5.0 ± 1.4	0.021 ± 0.002
CS91	90 ± 0.48	53 ± 20	5.1 ± 1.6	0.023 ± 0.001

Data represent mean ± standard deviation.

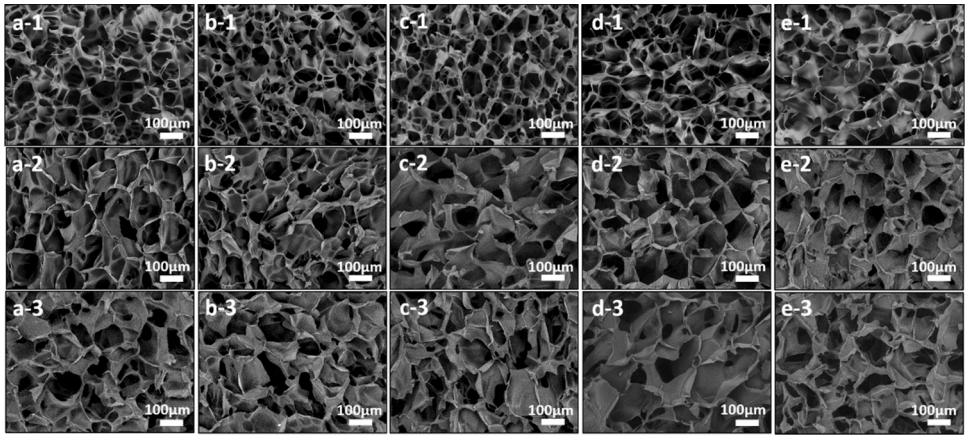

Fig. 1. Surface (1), cross section (2) and longitudinal section (3) of CS58 (a), CS73 (b), CS82 (c), CS88 (d) and CS91 (e) sponges evaluated by SEM.

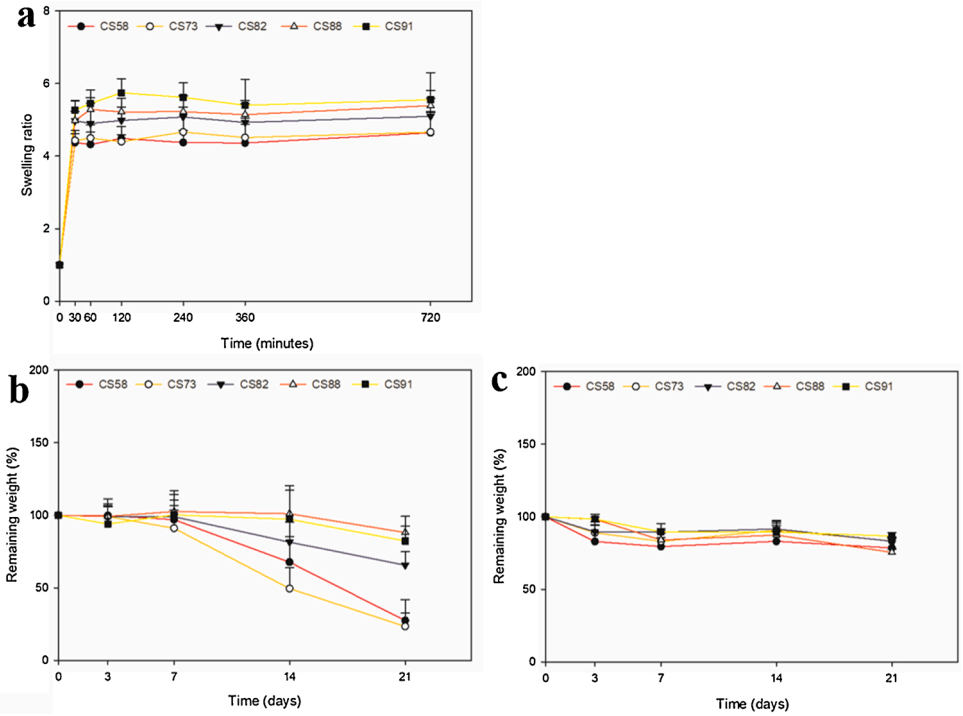

Fig. 2. Swelling ratio (a) and degradation behavior in lysozyme (b) and PBS (c) of chitosan sponges.

the CS88 sponges, and seen both in clusters and spread morphology (Fig. 3d). Numerous cells were attached on CS91 sponges as evidenced by the intensity of dye bound to the actin filaments. Cells spread with stretched actin filaments on the surface and across the pore walls. A number of pores were also filled with cells (Fig. 3e).

The LDH activity in the cell culture medium of osteoblasts cultured on the various chitosan sponges tested was lower than in control group on day 1 and day 3. On day 7, a slight increase in LDH activity was detected in the medium from CS58 and CS82 sponges, which later decreased on day 14. On day 21, the LDH activity increased for all sponge group but it was not statistically significant compared to control (Fig. 3g).

Small variations in caspase-3 activity in the cell culture media was found for all chitosan groups at the various time points tested. The caspase-3 activity was significantly lower in the medium of cells cultured on CS91 compared to control ($p < 0.05$) on day 1, which later increased slightly until the end of the test (Fig. 3h).

3.4. Bone markers and cytokines secreted in culture medium

Sponge groups with higher DDA, such as CS88 and CS91 sponges, induced an enhanced ALP activity in the cell culture media on day 3 compared to control; to 125 % ($p < 0.05$) and 160 % ($p < 0.001$), respectively. The activity was then reduced and it was significantly lower compared to control on day 21 ($p < 0.05$). The sponges with lower DDA did not induce any significant changes in the ALP activity in the cell culture medium at any time points. CS91 sponges induced a significant increase in ALP activity on day 3 compared to CS58 ($p < 0.001$) and CS73 ($p < 0.001$) sponges (Fig. 4a).

NHO cultures on chitosan sponges with lower DDA had an enhanced secretion of OPN on day 7, whereas sponges with higher DDA induced an enhanced secretion on days 14 and 21. CS58 and CS73 sponges induced an increased secretion to 210 % ($p = 0.001$) and 160 % ($p < 0.05$) compared to control on day 7, respectively and the secretion then subsided. OPN secretion induced by CS88 and CS91 sponges was lower at early time points, then found to be enhanced on day 14, and reached 190 % and 410 % increase, respectively, on day 21 ($p < 0.001$). CS91 sponges increased the secretion of OPN significantly on day 21 compared to other sponges ($p < 0.001$) (Fig. 4b).

Secretion of OPG was reduced for all groups on days 3 and 7 compared to control ($p < 0.05$). On day 14, CS58 and CS82 sponges induced an increase to 155 % ($p < 0.01$) and 130 % ($p < 0.05$), respectively, while the secretion from cells on the CS88 ($p < 0.05$) and CS91 ($p < 0.001$) sponges remained significantly lower compared to control. On day 21, OPG secretion was significantly reduced for all the sponges compared to control ($p < 0.0$). CS58 sponges increased the secretion of OPG significantly on day 14 compared to CS88 ($p < 0.05$) and CS91 ($p < 0.001$) sponges (Fig. 5a).

The secretion of SOST was not significantly changed from cells cultured on CS58 sponges on days 3 and 7, but showed an increase to 170 % ($p < 0.001$) on day 14. In contrast, the secretion of SOST to the media from cells cultures on CS82, CS88 and CS91 sponges were lower than control at all time points studied. CS58 sponges enhanced SOST secretion significantly on day 14 compared to CS88 ($p < 0.001$) and CS91 ($p < 0.05$) sponges (Fig. 5b).

DKK-1 secretion was lower compared to control at all time points for all groups of sponges tested. CS91 and CS88 sponges reduced the secretion significantly at each time point compared to control ($p < 0.001$). CS58 sponges increased DKK-1 secretion significantly at all time points compared to CS88 ($p < 0.001$) and CS91 ($p < 0.001$) sponges (Fig. 5c).

IL-6 secretion was enhanced by CS88 and reduced by CS91 sponges ($p < 0.05$) at early time points (days 3 and 7) compared to control. However, the secretion reached a significant increase on day 14 for both sponge groups, to 240 % by CS88 and 225 % by CS91 sponges ($p < 0.001$). Secretion was not significantly changed by other sponge groups when compared to control on day 14. CS88 and CS91 sponges enhanced the secretion of IL-6 significantly on day 14 compared to CS58 ($p < 0.001$) and CS73 sponges ($p < 0.001$) (Fig. 6a).

Secretion of MCP-1 to the medium from cells cultured on CS91 sponges was significantly lower compared to control ($p < 0.05$) while other sponge groups did not influence the secretion significantly on day 3. However, on day 7 all sponge groups induced a significantly reduced secretion of MCP-1 when compared to control ($p < 0.05$). CS91 reduced

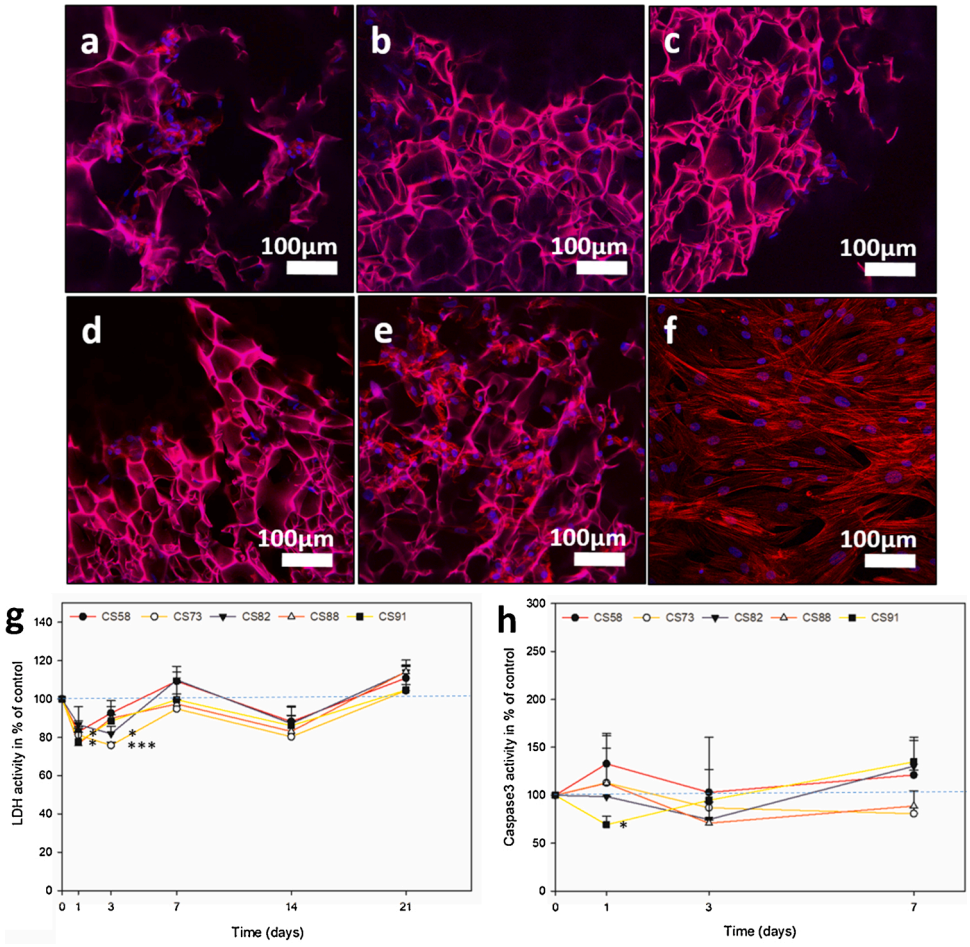

Fig. 3. Attachment of NHOs on CS58 (a), CS73 (b), CS82 (c), CS88 (d) and CS91 (e) sponges and plastic cell culture dishes (control;f) visualized by F-actin staining on day 3. LDH activity (g) and caspase-3 activity (h) in culture medium from NHOs seeded on chitosan sponges presented in percentage of control on days 1 and 3. Values represent the mean ± SD. Significantly different from control at *$p < 0.05$.

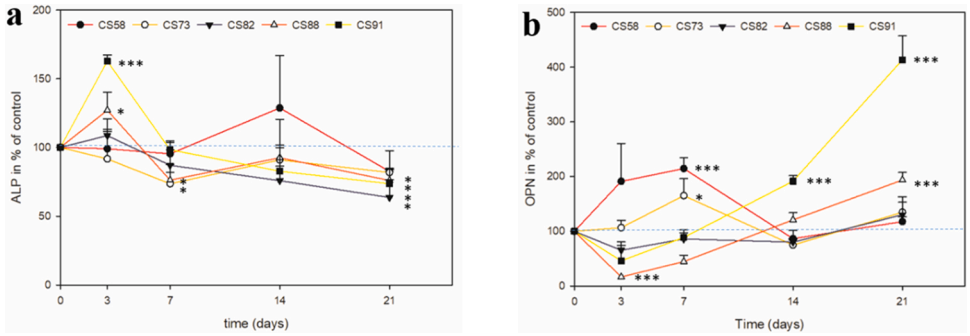

Fig. 4. Secretion of ALP (a) and OPN (b) in culture medium from NHOs seeded on chitosan sponges presented in percentage of levels found from cells cultured on plastic (control) on days 3, 7, 14 and 21. Values represent the mean ± SD. Significantly different from control at *$p < 0.05$ and ***$p < 0.001$.

the secretion of MCP-1 significantly on day 7 compared to other sponges ($p < 0.001$) (Fig. 6b).

Sponges with lower DDA did not show any specific trends in VEGF secretion. CS88 sponges enhanced the secretion on day 3 and reached 380 % increase on day 14 compared to control, then it decreased slightly ($p < 0.001$). Secretion induced by CS91 sponges was slightly higher than control at all time points and reached its highest level (170 % increase) on day 21 ($p < 0.05$). CS88 sponges enhanced the secretion of VEGF significantly on day 7, 14 and 21 compared to CS58 and CS73 sponges ($p < 0.001$) (Fig. 6c).

The overall variation in the secreted levels of bone markers and cytokines from osteoblasts cultured on the various chitosan sponges are illustrated in a heat map in Fig. 7.

4. Discussion

To the authors' knowledge, this is the first detailed analysis of the response from primary human osteoblasts to DDA and *Mw* of 3D sponges produced from various chitosan batches obtained from the same producer. DDA seemed to be the main characteristic of chitosan in determining the cell attachment behavior, regulating the secretion of bone markers and cytokines. However, the *Mw* also played an important role

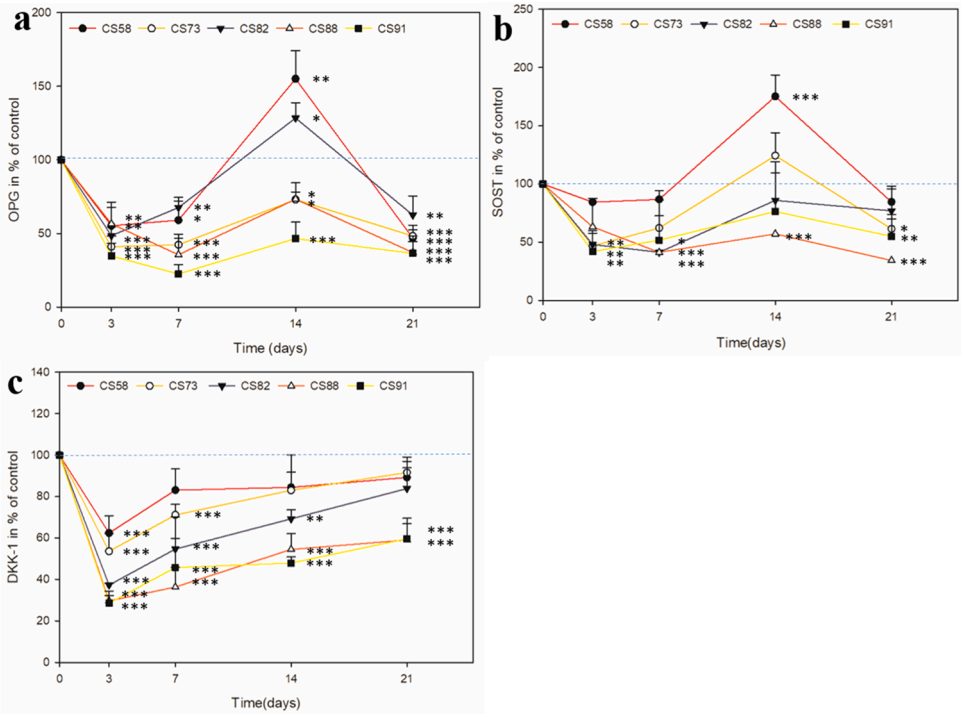

Fig. 5. Secretion of OPG (a), SOST (b) and DKK-1 (c) in culture medium from NHOs seeded on chitosan sponges presented in percentage of levels secreted from cells cultured on plastic (control) on days 3, 7, 14 and 21. Values represent the mean ± SD. Significantly different from control at *p < 0.05, **p < 0.01 and ***p < 0.001.

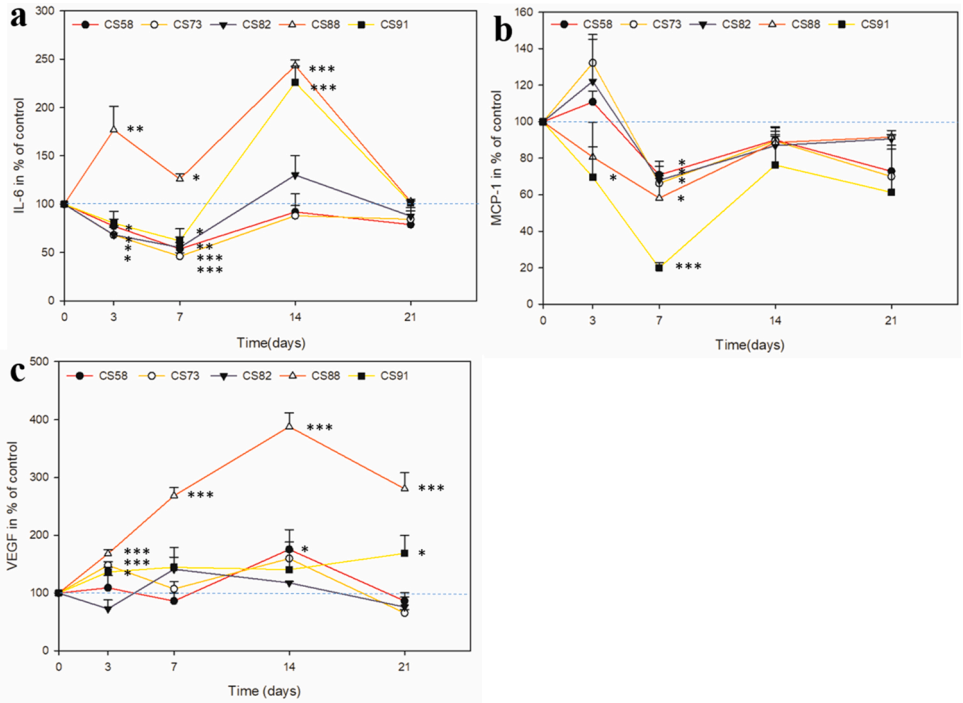

Fig. 6. Secretion of IL-6 (a), MCP-1 (b) and VEGF (c) in culture medium from NHOs seeded on chitosan sponges presented in percentage of levels secreted from cells cultured on plastic (control) on days 3, 7, 14 and 21. Values represent the mean ± SD. Significantly different from control at *p < 0.05, **p < 0.01 and ***p < 0.001.

in altering the number of cells attached and their differentiation behavior, although to a lesser extent.

The 3D porous sponges were fabricated from different batches of chitosan powders by freeze-drying. It is well known that the pore size, porosity and interconnectivity of a porous structure play important roles in regulating the aspects of cellular attachment, orientation, migration and function (Nguyen & Lee, 2014). Lu et al. reported that a minimum of 20 μm interconnected pores of hydroxyapatite and β-tricalcium phosphate scaffolds was required to allow osteoblast migration and a pore size greater than 40 μm facilitated cellular colonization and proliferation. However, to allow the bone ingrowth inside the macropores, the pore size must be over 50 μm (Lu et al., 1999). According to Nath et al.,

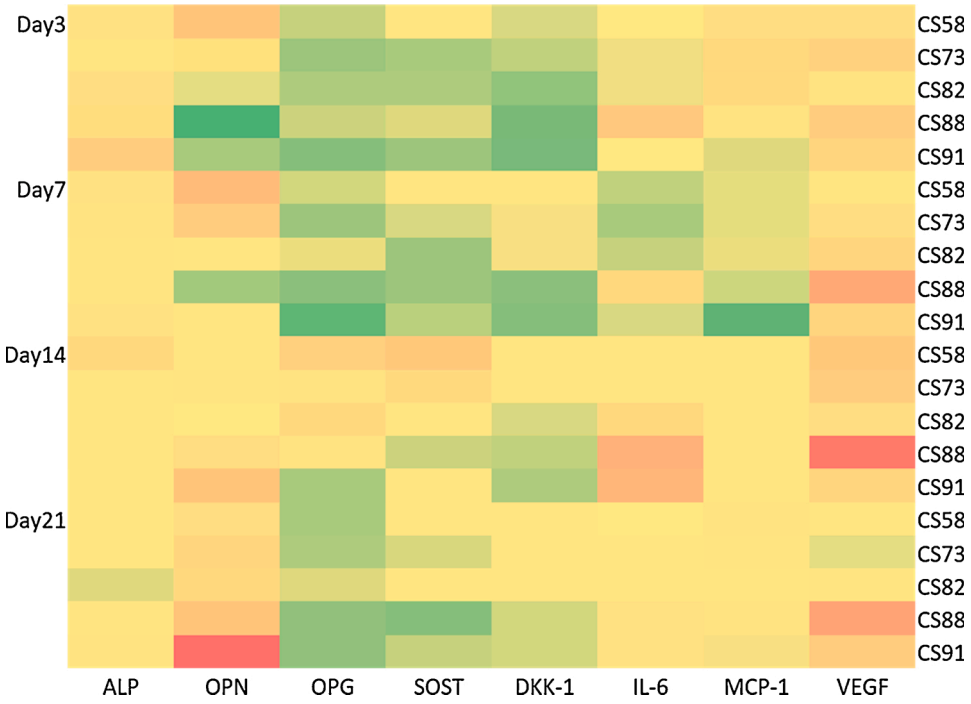

Fig. 7. Secretion levels of bone markers and cytokines in the culture medium. Red indicates highest value and green lowest value. (For interpretation of the references to colour in this figure legend, the reader is referred to the web version of this article).

chitosan–hyaluronic acid sponges with 75–87 % porosity and an average pore size of 50−90 μm supported migration and proliferation of osteoblasts (Nath et al., 2015). Amaral et al. prepared chitosan sponges with varied DDAs and determined the porosity, which ranged from 93 to 97% with the highest porosity value for the DDA of 51 % and an average pore size values ranging from 61−87 μm. They did not, however, find any significant correlation between the DDA, and sponge porosity and pore size (Amaral, Sampaio, & Barbosa, 2006). In our study, the porosity of the fabricated sponges was 90–94 %, and not related to the variation in DDA (58–91 %) or M_W (749−170 kDa) of the chitosan batches tested, however the pore size of the sponges ranged from 53−88 μm where the lowest pore size was presented by the CS91 sponges.

Lamella thickness is another crucial parameter in relation to the mechanical strength and pore size of a 3D porous structure. Xia et al. created collagen–apatite scaffolds with different lamella thickness ranging from 3.6–23 μm. Thick lamellae increased the mechanical strength, whereas, thin lamellae increased pore size of the scaffolds (Xia, Villa, & Wei, 2014). The lamella thickness of the sponges in our study was similar (5 μm) for all sponge groups. Mechanical properties of a porous structure is an important aspect with regard to cell-material interactions. A material should be mechanically strong to support cell adhesion, communication and function (Khalili & Ahmad, 2015; Trembecka-Wójciga et al., 2020). This study showed that the mechanical strength of the sponges was inversely correlated to DDA.

Degradation of chitosan is dependent on degree of distribution of amino groups on the side chains. In this study, lower DDA chitosan was degraded more rapidly than higher DDA chitosan, which is supported by previous studies (Islam, Dmour, & Taha, 2019; Zhou et al., 2008).

All chitosan sponge groups were non-cytotoxic and supported cell attachment. Cell spreading was higher while increasing the DDA. These results support a previous study which revealed that increased number of amino groups on the surface of higher DDA sponges favor the cell spreading through their interaction with negatively charged cell membrane (Amaral et al., 2006). Interestingly, there was a considerable difference in the cell attachment behavior between the sponges with higher DDA. Numerous cells were attached on CS91 sponges, spreading along and across the sponge walls with long filopodia and higher number of cell-to-cell contact. While there was no significant difference in the sponge architecture among different chitosan batches, the other characteristics might contribute to alter the cell attachment behavior. Tangsadthakun et al. showed that the effect of different M_W on cell attachment and proliferation behavior on chitosan was intrinsically dependent on its interaction with secreted cell proteins response for maintaining the microenvironment for L929 cell growth (Tangsadthakun et al., 2007).

On the cellular level, ALP is the most recognized osteogenic marker. Stein et al. found that the expression of ALP started when osteoblasts ceased to proliferate, reached its maximum during matrix maturation and declined when matrix mineralization started (Stein, Lian, & Owen, 1990). Amaral et al. tested ALP activity of MG-63 cells cultured on the chitosan sponge groups with various DDA and found no significant difference between any of the groups (Amaral et al., 2006). However, in our study, early increased activity of ALP was enhanced with high DDA. M_W did not seem to alter the secretion. Following the proliferative period, OPN, another bone related protein, is expressed and reached a peak during mineralization (Stein et al., 1989; Yoon, Buenaga, & Rodan, 1987). Our findings indicate that lower DDA sponges induced the secretion of OPN at early time points while higher DDA sponges enhanced the secretion at late time points. The notable difference in the secretion on day 21 between the two groups of sponges with higher DDA might be due to the difference in M_W. OPG is a secreted protein involved in the regulation of bone density by inhibiting osteoclastogenesis and associated bone resorption (Lacey et al., 1998; Simonet et al., 1997). DKK-1 and SOST, however, secreted by the osteoblasts act as negative regulators of bone mass inhibiting the signaling pathways required for enhanced bone formation (Kamiya, 2012). In this study, lower DDA sponges enhanced the secretion of OPG and SOST on day 14. Changes in M_W did not show any significant influence in the secretion of OPG, SOST and DKK-1. These results indicate that high DDA may facilitate osteoblast differentiation and extracellular matrix production, whereas low DDA stimulates the secretion of factors supporting octeoclastogenesis.

IL-6 plays a dual role in bone remodeling. IL-6 enhances the in vitro differentiation of osteoblast precursors isolated from the calvaria or bone marrow (Blanchard et al., 2009; Erices et al., 2002; Franchimont,

Wertz, & Malaise, 2005). On the other hand, it stimulates the formation of multinucleated cells expressing the osteoclast phenotypes in human bone marrow cultures (Ishimi et al., 1990; Kurihara et al., 1989). MCP-1 is another enhancer of osteoclast differentiation. RANKL induced MCP-1 promotes osteoclast fusion into multinuclear cells responsible for bone resorption (Kim, Day, & Morrison, 2005). Barbosa et al. implanted chitosan porous scaffolds with DDAs of 85 and 94 % subcutaneously in a BALB/c mice model. chitosan with 85 % DDA attracted the higher numbers of polymorphonuclear leukocytes to the defect site initially and presented higher numbers of adherent inflammatory cells after 4 weeks of implantation (Barbosa et al., 2010). In this study, inflammatory cytokine IL-6 secretion was increased for higher DDA sponges. CS88 sponges enhanced the secretion of IL-6 both at early and late time points while CS91 sponges increased the secretion on day 14 only. The endotoxin content was higher in CS88 sponges than in CS91 sponges (Table 1) which might be responsible for the increased early stage IL-6 secretion. Chitosan are known to bind substantial amounts of endotoxin (Davydova et al., 2000). This residual endotoxin has been demonstrated to significantly influence cellular interaction with chitosan (Lieder et al., 2013; Nolte et al., 2014; Ravindranathan et al., 2016). Lieder et al. reported a significant increase in IL-6 secretion from human bone marrow-derived mesenchymal stem cells in the presence of endotoxins in chitosan derivatives on day 3 and 7 (Lieder et al., 2013). Secretion of MCP-1 was decreased for all sponges on day 7. However, the secretion was markedly lower for CS91 than CS88 sponges. Variation in the M_W and endotoxin content of the chitosan batches with similar DDA might cause the difference in the secretion pattern. VEGF is an essential signaling molecule for angiogenesis. Inactivation of VEGF causes almost complete suppression of blood vessel invasion in newly growing bones resulting in reduced bone lengthening (Gerber et al., 1999). Xu et al. studied the effect of chitosan nanoparticles (CNP) on tumor angiogenesis in nude mice model. They claimed that CNP inhibited angiogenesis of human hepatocellular carcinoma (HCC) by suppressing VEGF receptor 2 expression. CNP had no effect on VEGF mRNA and protein expression of HCC (BEL-7402) cells. (Xu, Wen, & Xu, 2009). In our study, chitosan sponges with lower DDA showed similar results. The sponges with higher DDA (CS88 and CS91), however, enhanced the secretion of VEGF where greater increase caused by CS88 might be the result of higher M_W. These results indicate that sponges with high molecular weight may facilitate the osteoblasts to secrete factors inducing angiogenesis and bone remodeling.

The objective of this study was to determine how DDA and *Mw* affected the biological properties of chitosan sponges. In the process of deacetylation, the acetyl groups on chitosan side chains are transformed to the primary amino groups. Varying the DDA influences many other chitosan properties, such as surface charge, degradation, hydrophilicity, crystallinity and elongation (Hsu et al., 2004; Yuan et al., 2011). Again, greater tensile strength and moisture adsorption is attributed to higher *Mw* of chitosan (Hsu et al., 2004; Nunthanid et al., 2001). We hypothesize that, these parameters alone or by combined interactions might play significant roles in altering the biological response of chitosan sponges.

5. Conclusions

Highly porous chitosan sponges were produced from different chitosan batches by freeze-drying. Low DDA chitosan sponges had a higher mechanical strength and higher degradation rate than those with high DDA. High DDA chitosan favored osteoblast attachment and cell spreading, as well as the secretion of bone markers indicating enhanced osteoblast differentiation and extracellular matrix production whereas low DDA induced secretion of factors promoting osteoclastogensis. High molecular weight, on the other hand, was found to induce the secretion of factors facilitating angiogenesis and bone remodeling.

The variations in cellular responses to the different chitosan sponges indicate a potential for individual tailoring of desired responses in guided bone regeneration.

CRediT authorship contribution statement

Mousumi Sukul: Conceptualization, Methodology, Writing - original draft. **Priyanka Sahariah:** Methodology, Writing - review & editing. **Hélène L. Lauzon:** Funding acquisition, Methodology, Resources, Writing - review & editing. **João Borges:** Funding acquisition, Validation, Writing - review & editing. **Már Másson:** Funding acquisition, Methodology, Writing - review & editing. **João F. Mano:** Funding acquisition, Validation, Writing - review & editing. **Håvard J. Haugen:** Funding acquisition, Validation, Writing - review & editing. **Janne E. Reseland:** Funding acquisition, Conceptualization, Methodology, Writing - review & editing, Supervision.

Declaration of Competing Interest

The authors report no declarations of interest.

Acknowledgements

This work was supported by The Marine Biotechnology ERA-NET project, “Blueteeth” (ERA-MBT/0002/2015) financed under EU FP7 (Grant Agreement number: 604814). This is a co-funded project coordinated by the University of Aveiro, Portugal (supported by the Portuguese Foundation for Science and Technology (FCT)), and having the company Primex ehf and University of Iceland, Iceland (supported by the Icelandic Technical Development Fund grant No. 179012-0612) and the University of Oslo, Norway (supported by the Norway Research Council, Project ID 269522/O70) as partners. This work was developed within the scope of the project CICECO – Aveiro Institute of Materials, UIDB/50011/2020 & UIDP/50011/2020, financed by national funds through the Foundation for Science and Technology/MCTES. J. Borges gratefully acknowledges the financial support by FCT through his individual contract (CEECIND/03202/2017). The authors would like to thank Aina-Mari Lian for the contribution in Luminex experiment and Liebert Parreiras Nogueira for nano CT analyses and, and Dr. Svetlana Solodova for assistance with the GPC analysis.

Appendix A. Supplementary data

Supplementary material related to this article can be found, in the online version, at doi:https://doi.org/10.1016/j.carbpol.2020.117434.

References

Alves, N. M., & Mano, J. F. (2008). Chitosan derivatives obtained by chemical modifications for biomedical and environmental applications. *International Journal of Biological Macromolecules, 43*(5), 401–414.

Amaral, I., Sampaio, P., & Barbosa, M. (2006). Three-dimensional culture of human osteoblastic cells in chitosan sponges: The effect of the degree of acetylation. *Journal of Biomedical Materials Research Part A: An Official Journal of The Society for Biomaterials, The Japanese Society for Biomaterials, and The Australian Society for Biomaterials and the Korean Society for Biomaterials, 76*(2), 335–346.

Austin, P., et al. (1981). Chitin: New facets of research. *Science, 212*(4496), 749–753.

Barbosa, J. N., et al. (2010). Evaluation of the effect of the degree of acetylation on the inflammatory response to 3D porous chitosan scaffolds. *Journal of Biomedical Materials Research Part A: An Official Journal of The Society for Biomaterials, The Japanese Society for Biomaterials, and The Australian Society for Biomaterials and the Korean Society for Biomaterials, 93*(1), 20–28.

Berger, J., et al. (2004). Structure and interactions in covalently and ionically crosslinked chitosan hydrogels for biomedical applications. *European Journal of Pharmaceutics and Biopharmaceutics, 57*(1), 19–34.

Bhattacharya, M., et al. (2012). Nanofibrillar cellulose hydrogel promotes three-dimensional liver cell culture. *Journal of Controlled Release, 164*(3), 291–298.

Blanchard, F., et al. (2009). The dual role of IL-6-type cytokines on bone remodeling and bone tumors. *Cytokine & Growth Factor Reviews, 20*(1), 19–28.

Chandy, T., & Sharma, C. P. (1990). Chitosan-as a biomaterial. *Biomaterials, Artificial Cells, and Artificial Organs, 18*(1), 1–24.

Chatelet, C., Damour, O., & Domard, A. (2001). Influence of the degree of acetylation on some biological properties of chitosan films. *Biomaterials, 22*(3), 261–268.

Chenite, A., et al. (2000). Novel injectable neutral solutions of chitosan form biodegradable gels in situ. *Biomaterials, 21*(21), 2155–2161.
Cheung, R. C. F., et al. (2015). Chitosan: An update on potential biomedical and pharmaceutical applications. *Marine Drugs, 13*(8), 5156–5186.
Cho, Y. I., No, H. K., & Meyers, S. P. (1998). Physicochemical characteristics and functional properties of various commercial chitin and chitosan products. *Journal of Agricultural and Food Chemistry, 46*(9), 3839–3843.
Christensen, B. E., Vold, I. M. N., & Vårum, K. M. (2008). Chain stiffness and extension of chitosans and periodate oxidised chitosans studied by size-exclusion chromatography combined with light scattering and viscosity detectors. *Carbohydrate Polymers, 74*(3), 559–565.
Costa, A. M., & Mano, J. F. (2015). Highly robust hydrogels via a fast, simple and cytocompatible dual crosslinking-based process. *Chemical Communications, 51*(86), 15673–15676.
Croisier, F., & Jérôme, C. (2013). Chitosan-based biomaterials for tissue engineering. *European Polymer Journal, 49*(4), 780–792.
Custódio, C. A., et al. (2015). Cell selective chitosan microparticles as injectable cell carriers for tissue regeneration. *Biomaterials, 43*, 23–31.
Davydova, V., et al. (2000). Interaction of bacterial endotoxins with chitosan. Effect of endotoxin structure, chitosan molecular mass, and ionic strength of the solution on the formation of the complex. *Biochemistry C/C of Biokhimiia, 65*(9), 1082–1090.
Di Martino, A., Sittinger, M., & Risbud, M. V. (2005). Chitosan: A versatile biopolymer for orthopaedic tissue-engineering. *Biomaterials, 26*(30), 5983–5990.
Eiselt, P., et al. (2000). Porous carriers for biomedical applications based on alginate hydrogels. *Biomaterials, 21*(19), 1921–1927.
Erices, A., et al. (2002). gp130 Activation by soluble interleukin-6 receptor/interleukin-6 enhances osteoblastic differentiation of human bone marrow-derived mesenchymal stem cells. *Experimental Cell Research, 280*(1), 24–32.
Foster, L. J. R., et al. (2015). Chitosan as a biomaterial: Influence of degree of deacetylation on its physiochemical, material and biological properties. *PloS One, 10*(8). e0135153.
Franchimont, N., Wertz, S., & Malaise, M. (2005). Interleukin-6: An osteotropic factor influencing bone formation? *Bone, 37*(5), 601–606.
Francis Suh, J. K., & Matthew, H. W. T. (2000). Application of chitosan-based polysaccharide biomaterials in cartilage tissue engineering: A review. *Biomaterials, 21*(24), 2589–2598.
Garcia Cruz, D. M., et al. (2010). Differentiation of mesenchymal stem cells in chitosan scaffolds with double micro and macroporosity. *Journal of Biomedical Materials Research Part A, 95*(4), 1182–1193.
Gerber, H.-P., et al. (1999). VEGF couples hypertrophic cartilage remodeling, ossification and angiogenesis during endochondral bone formation. *Nature Medicine, 5*(6). p. 623.
Hamilton, V., et al. (2007). Bone cell attachment and growth on well-characterized chitosan films. *Polymer International, 56*(5), 641–647.
Han, L., et al. (2014). BMP2-encapsulated chitosan coatings on functionalized Ti surfaces and their performance in vitro and in vivo. *Materials Science and Engineering C, 40*, 1–8.
Han, F., et al. (2017). Chitosan-gelatin hydrogel/PLGA scaffold with dual-delivery of TGF-β1 and BMP-2 for osteochondral defect repair. *Journal of Controlled Release, 259*, e34–e35.
Hoemann, C. D., et al. (2005). Tissue engineering of cartilage using an injectable and adhesive chitosan-based cell-delivery vehicle. *Osteoarthritis and Cartilage, 13*(4), 318–329.
Hollister, S. J. (2005). Porous scaffold design for tissue engineering. *Nature Materials, 4*(7), 518–524.
Hsu, S.-h., et al. (2004). Chitosan as scaffold materials: Effects of molecular weight and degree of deacetylation. *Journal of Polymer Research, 11*(2), 141–147.
Ishimi, Y., et al. (1990). IL-6 is produced by osteoblasts and induces bone resorption. *The Journal of Immunology, 145*(10), 3297–3303.
Islam, N., Dmour, I., & Taha, M. O. (2019). Degradability of chitosan micro/nanoparticles for pulmonary drug delivery. *Heliyon, 5*(5), e01684.
Kamiya, N. (2012). The role of BMPs in bone anabolism and their potential targets SOST and DKK1. *Current Molecular Pharmacology, 5*(2), 153–163.
Kean, T., & Thanou, M. (2010). Biodegradation, biodistribution and toxicity of chitosan. *Advanced Drug Delivery Reviews, 62*(1), 3–11.
Khalili, A. A., & Ahmad, M. R. (2015). A review of cell adhesion studies for biomedical and biological applications. *International Journal of Molecular Sciences, 16*(8), 18149–18184.
Khor, E., & Lim, L. Y. (2003). Implantable applications of chitin and chitosan. *Biomaterials, 24*(13), 2339–2349.
Kim, M. S., Day, C. J., & Morrison, N. A. (2005). MCP-1 is induced by RANKL, promotes human osteoclast fusion and rescues GM-CSF suppression of osteoclast formation. *The Journal of Biological Chemistry, 280*, 16163–16169.
Kim, B.-R., et al. (2014). In vitro and in vivo studies of BMP-2-loaded PCL–gelatin–BCP electrospun scaffolds. *Tissue Engineering Part A, 20*(23–24), 3279–3289.
Kumar, P., et al. (2020). Fabrication and characterization of silver nanorods incorporated calcium silicate scaffold using polymeric sponge replica technique. *Materials & Design, 195*. p. 109026.
Kurihara, N., et al. (1989). Interleukin 6 (IL-6) stimulates osteoclast formation in vitro by inducing IL-1 production. *Experimental Hematology, 17*. p. 577.
Lacey, D. L., et al. (1998). Osteoprotegerin ligand is a cytokine that regulates osteoclast differentiation and activation. *Cell, 93*(2), 165–176.
Li, Q., et al. (1992). Applications and properties of chitosan. *Journal of Bioactive and Compatible Polymers, 7*(4), 370–397.
Li, F., et al. (2014). Porous chitosan bilayer membrane containing TGF-β1 loaded microspheres for pulp capping and reparative dentin formation in a dog model. *Dental Materials, 30*(2), 172–181.
Lieder, R., et al. (2012). In vitro bioactivity of different degree of deacetylation chitosan, a potential coating material for titanium implants. *Journal of Biomedical Materials Research Part A, 100*(12), 3392–3399.
Lieder, R., et al. (2013). Endotoxins affect bioactivity of chitosan derivatives in cultures of bone marrow-derived human mesenchymal stem cells. *Acta Biomaterialia, 9*(1), 4771–4778.
Liu, Z., et al. (2020). Fabrication and energy absorption ability of 3D highly elastic sponge constructed by BN fiber balls. *Ceramics International*.
Liu Tsang, V., & Bhatia, S. N. (2004). Three-dimensional tissue fabrication. *Advanced Drug Delivery Reviews, 56*(11), 1635–1647.
Loh, Q. L., & Choong, C. (2013). Three-dimensional scaffolds for tissue engineering applications: Role of porosity and pore size. *Tissue Engineering Part B: Reviews, 19*(6), 485–502.
Lu, J., et al. (1999). Role of interconnections in porous bioceramics on bone recolonization in vitro and in vivo. *Journal of Materials Science Materials in Medicine, 10*(2), 111–120.
Monteiro, O. A. C., & Airoldi, C. (1999). Some studies of crosslinking chitosan–glutaraldehyde interaction in a homogeneous system. *International Journal of Biological Macromolecules, 26*(2), 119–128.
Muzzarelli, R. A. A. (1993). Biochemical significance of exogenous chitins and chitosans in animals and patients. *Carbohydrate Polymers, 20*(1), 7–16.
Muzzarelli, R. A. A. (2009). Genipin-crosslinked chitosan hydrogels as biomedical and pharmaceutical aids. *Carbohydrate Polymers, 77*(1), 1–9.
Muzzarelli, R. A. A., Lough, C., & Emanuelli, M. (1987). The molecular weight of chitosans studied by laser light-scattering. *Carbohydrate Research, 164*, 433–442.
Nath, S. D., et al. (2015). Chitosan–hyaluronic acid polyelectrolyte complex scaffold crosslinked with genipin for immobilization and controlled release of BMP-2. *Carbohydrate Polymers, 115*, 160–169.
Nguyen, T. B. L., & Lee, B.-T. (2014). A combination of biphasic calcium phosphate scaffold with hyaluronic acid-gelatin hydrogel as a new tool for bone regeneration. *Tissue Engineering Part A, 20*(13-14), 1993–2004.
Nolte, A., et al. (2014). Endotoxins affect diverse biological activity of chitosans in matters of hemocompatibility and cytocompatibility. *Journal of Materials Science Materials in Medicine, 25*(9), 2121–2130.
Nunthanid, J., et al. (2001). Physical properties and molecular behavior of chitosan films. *Drug Development and Industrial Pharmacy, 27*(2), 143–157.
Rabea, E. I., et al. (2003). Chitosan as antimicrobial agent: Applications and mode of action. *Biomacromolecules, 4*(6), 1457–1465.
Ravindranathan, S., et al. (2016). Effect of chitosan properties on immunoreactivity. *Marine Drugs, 14*(5). p. 91.
Rezaii, M., Oryan, S., & Javeri, A. (2019). Curcumin nanoparticles incorporated collagen-chitosan scaffold promotes cutaneous wound healing through regulation of TGF-β1/Smad7 gene expression. *Materials Science and Engineering C, 98*, 347–357.
Riksen, E. A., et al. (2011). Human osteoblastic cells discriminate between 20-kDa amelogenin isoforms. *European Journal of Oral Sciences, 119*, 357–365.
Rinaudo, M., Milas, M., & Le Dung, P. (1993). Characterization of chitosan. Influence of ionic strength and degree of acetylation on chain expansion. *International Journal of Biological Macromolecules, 15*(5), 281–285.
Rong Huei, C., & Hwa, H.-D. (1996). Effect of molecular weight of chitosan with the same degree of deacetylation on the thermal, mechanical, and permeability properties of the prepared membrane. *Carbohydrate Polymers, 29*(4), 353–358.
Simonet, W. S., et al. (1997). Osteoprotegerin: A novel secreted protein involved in the regulation of bone density. *Cell, 89*(2), 309–319.
Stein, S. G., et al. (1989). The onset and progression of osteoblast differentiation is functionally related to cellular proliferation. *Connective Tissue Research, 20*(1–4), 3–13.
Stein, G. S., Lian, J. B., & Owen, T. A. (1990). Relationship of cell growth to the regulation of tissue-specific gene expression during osteoblast differentiation. *The FASEB Journal, 4*(13), 3111–3123.
Stie, M. B., et al. (2020). Swelling of mucoadhesive electrospun chitosan/polyethylene oxide nanofibers facilitates adhesion to the sublingual mucosa. *Carbohydrate Polymers, 242*. p. 116428.
Tangsadthakun, C., et al. (2007). The influence of molecular weight of chitosan on the physical and biological properties of collagen/chitosan scaffolds. *Journal of Biomaterials Science Polymer Edition, 18*(2), 147–163.
Terbojevich, M., et al. (1991). Chitosan: chain rigidity and mesophase formation. *Carbohydrate Research, 209*, 251–260.
Tiraferri, A., et al. (2014). Mechanism of chitosan adsorption on silica from aqueous solutions. *Langmuir, 30*(17), 4980–4988.
Trembecka-Wójciga, K., et al. (2020). Effect of the mechanical properties of carbon-based coatings on the mechanics of cell–material interactions. *Colloids and Surfaces B: Biointerfaces*. p. 111359.
Wang, C., et al. (2020). 3D printing of bone tissue engineering scaffolds. *Bioactive Materials, 5*(1), 82–91.
Wenling, C., et al. (2005). Effects of the degree of deacetylation on the physicochemical properties and schwann cell affinity of chitosan films. *Journal of Biomaterials Applications, 20*(2), 157–177.
Xia, Z., Villa, M., & Wei, M. (2014). A biomimetic collagen–apatite scaffold with a multi-level lamellar structure for bone tissue engineering. *Journal of Materials Chemistry B, 2*(14), 1998–2007.
Xu, Y., Wen, Z., & Xu, Z. (2009). Chitosan nanoparticles inhibit the growth of human hepatocellular carcinoma xenografts through an antiangiogenic mechanism. *Anticancer Research, 29*(12), 5103–5109.

Yoon, K., Buenaga, R., & Rodan, G. A. (1987). Tissue specificity and developmental expression of rat osteopontin. *Biochemical and Biophysical Research Communications, 148*(3), 1129–1136.

Yuan, Y., et al. (2011). Deacetylation of chitosan: Material characterization and in vitro evaluation via albumin adsorption and pre-osteoblastic cell cultures. *Materials (Basel, Switzerland), 4*(8), 1399–1416.

Zaharoff, D. A., et al. (2007). Chitosan solution enhances both humoral and cell-mediated immune responses to subcutaneous vaccination. *Vaccine, 25*(11), 2085–2094.

Zhang, H., & Neau, S. H. (2001). In vitro degradation of chitosan by a commercial enzyme preparation: effect of molecular weight and degree of deacetylation. *Biomaterials, 22*(12), 1653–1658.

Zhao, H., et al. (2018). Effect of porous structure and pore size on mechanical strength of 3D-printed comby scaffolds. *Materials Letters, 223*, 21–24.

Zhou, H. Y., et al. (2008). Effect of molecular weight and degree of chitosan deacetylation on the preparation and characteristics of chitosan thermosensitive hydrogel as a delivery system. *Carbohydrate Polymers, 73*(2), 265–273.